

ORIGINAL  
RESEARCH

X.-Q. Ding  
Y. Sun  
H. Braaß  
T. Illies  
H. Zeumer  
H. Lanfermann  
J. Fiehler

# Evidence of Rapid Ongoing Brain Development Beyond Two Years of Age Detected by Fiber Tracking

**BACKGROUND AND PURPOSE:** Development of callosal fibers is important for psychomotor and cognitive functions. We hypothesized that brain maturation changes are detectable beyond 2 years of age by using diffusion tensor imaging (DTI) of the corpus callosum (CC).

**MATERIALS AND METHODS:** T2 and fractional anisotropy (FA) maps of the brain of 55 healthy subjects between 0.2 and 39 years of age were obtained. Quantitative T2 and FA values were measured at the genu and splenium of the CC (gCC and sCC). Fiber tracking, volumetric determination, and the fiber density calculations of the CC were related to age. A paired *t* test was used for significant differences between the values at the gCC and sCC.

**RESULTS:** T2 relaxation times at gCC and sCC decrease fast in the first months of life and very little after 2 years of age. The FA<sub>gCC</sub> increases until 5 years of age and remains nearly constant thereafter; it showed a significant increase from 0 to 2 years versus 2–5 years, whereas there was no difference in the other age groups. FA<sub>sCC</sub> values showed no significant changes after 2 years of age. The fiber density of the CC shows a tendency of inverse age dependence from childhood to adulthood.

**CONCLUSION:** Rapid ongoing changes in brain maturation (increase in FA<sub>gCC</sub>) are detectable until 5 years of age. DTI reveals more information about brain maturation than T2 relaxometry.

Early human brain development is of considerable clinical relevance because many neurologic and neurobehavioral disorders originate from early disturbances during structural and functional cerebral maturation. The degree of maturation and its deviation from a normal course in clinical practice are determined by visual inspection of MR images and a comparison with milestones revealed on MR imaging, such as the consecutive myelination of certain brain structures.<sup>1</sup> The monitoring of quantitative MR imaging parameters allows a more objective estimation of normal or pathologic brain development as a useful adjunct to this method.<sup>2–6</sup> Recent data suggest that brain maturation still persists during adolescence.<sup>7–9</sup> The corpus callosum (CC), the largest and most prominent axonal pathway, functions to connect left and right cerebral hemispheres. Callosal fibers are important for motor and sensory integration, attention, memory, and general cognitive functioning. Any disturbance could lead to clinical impairment.<sup>10–12</sup> Despite the great interest in the development and function of interhemispheric connections, little is known about the development and organization of the tract itself.<sup>13–17</sup> Previous studies, including those of children of different age ranges, found age-dependent fractional anisotropy (FA) values.<sup>8,9,18,19</sup> A monitoring method for the normal maturation progress covering a wider age range may provide the basis for

detection of deviations under pathologic conditions and may support routine diagnostics as an objective auxiliary tool.

In the present work, we studied the age-dependent development of the CC in infants, children, and adults by using MR relaxometric and volumetric methods as well as diffusion tensor imaging (DTI) under routine imaging conditions. We hypothesized that brain maturation changes are detectable in the CC by using DTI beyond 2 years of age.

## Methods

**Subjects.** Fifty-five subjects were studied in 2 cohorts: An adult group consisted of 20 healthy volunteers, 20–39 years of age (9 men, 11 women). We enrolled 35 children and adolescents (20 male, 15 female) with an age range of 2 months to 15 years, subdivided into 4 age groups (0–2 years, *n* = 9; >2–5 years, *n* = 7; >5–10 years, *n* = 14; >10–15 years, *n* = 5), who were retrospectively selected from a pool of 850 pediatric patients examined by MR imaging as a part of routine diagnostic procedures related to numerous pediatric investigations. Patients with any brain lesions or brain abnormalities on conventional MR imaging were excluded. Only children without abnormal MR imaging findings, with no clinical signs of brain anomalies, fever, or acute infection determined independently by 2 experienced neuroradiologists, were included. The local medical ethics committee approved the study. Informed consent was obtained from healthy volunteers and the parents of the children.

**MR Imaging Protocol.** All MR imaging studies were performed on a 1.5T system (Sonata; Siemens, Erlangen, Germany) with a standard quadrature head coil. The routinely applied protocol consisted of a sagittal T1-weighted 3D magnetization-prepared rapid acquisition of gradient echo (MPRAGE) sequence; a transversal proton/T2-weighted triple-echo turbo spin-echo (TSE) sequence, which acquires images at 3 different echo times (14, 71, and 128 ms); a sagittal T2-weighted TSE sequence; and a transversal single-shot spin-echo echo-planar imaging sequence with 6 motion-probing gradients (*b* = 0, 1500 s/mm<sup>2</sup>) for DTI.<sup>20,21</sup> A 20-cm<sup>2</sup> FOV for children and a 23 cm<sup>2</sup>

Received December 12, 2007; accepted after revision February 19, 2008.

From the Department of Neuroradiology (X.-Q.D., Y.S., H.B., T.I., H.Z., J.F.), University Medical Center Hamburg-Eppendorf, University of Hamburg, Hamburg, Germany; and the Institute of Diagnostic and Interventional Neuroradiology (X.-Q.D., H.L.), Hannover Medical School, Hannover, Germany.

This work was financially supported by the Federal Ministry of Education and Research (BMBF) under the grant number 01GM0309.

Please address correspondence to: Xiao-Qi Ding, PhD, MD, Institute of Diagnostic and Interventional Neuroradiology, Hannover Medical School, Carl-Neuberg-Str 1, 30625 Hannover, Germany; e-mail: Ding.Xiaoqi@mh-hannover.de

DOI 10.3174/ajnr.A1097

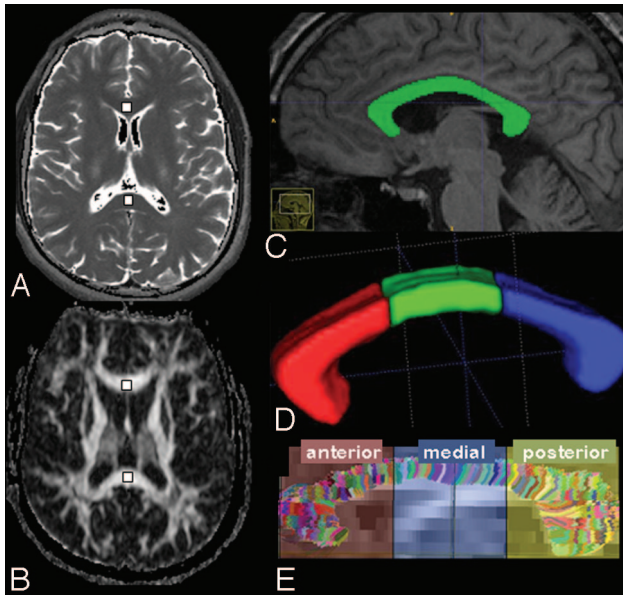


**Fig 1.** A, T2 map (anterior is at the top) at the horizontal level of the striatum containing the gCC and sCC, derived from a triple-echo sequence. B, Corresponding FA map. The rectangles are the regions of interest. C, The anatomic structure of the CC displayed in an MPRAGE image. D, The volume of the CC obtained with software InsightSNAPS. E, Fiber of the CC obtained by fiber tracking with DTIStudio software.

FOV for the adult cohort were used with a  $256 \times 256$  matrix size for MPRAGE sequences; a  $192 \times 256$  matrix size for TSE sequences; and a  $96 \times 128$  matrix size for DTI sequence. Section thickness without intersection gap for DTI was 3 mm; for MPRAGE, 1 mm; and for all others, 5 mm. All raw data were reconstructed into a display matrix of  $256 \times 256$  pixels. The table scanning time was approximately 22 minutes.

**Data Analysis.** Brain maps of the T2 relaxation times (T2) of all subjects were obtained by using a software implemented on the MR imaging console (courtesy of Dr. Finsterbusch, NeuroImage Nord, Hamburg, Germany), by using a nonlinear least-squares fit from the 3 images acquired with the triple-echo TSE sequence.<sup>7</sup> FA maps were obtained by using a DTI task card implemented on the MR imaging console (courtesy of Dr. Sorensen, Massachusetts General Hospital, Boston, Mass). The numeric values of T2 and FA of the genu and splenium of the CC (FAGCC and FAsCC) were measured off-line in 2 distinctive regions of interest—one at the gCC and the other at the sCC—by using the routine viewer software eFilm (Merge eMed, Milwaukee, Wis) (Fig 1A, B). Both regions of interest were carefully chosen to minimize the partial volume effects and were drawn manually as a square of  $20 \pm 2 \text{ mm}^2$ . The reported numeric values represent the mean values of 3 repeated measurements. Fiber tracking of the brain was performed by using DTIStudio software with determination of the fiber number of the CC (Fig 1E).<sup>22</sup> Finally, the volume of the CC (Fig 1C, D) was determined on the basis of 3D MPRAGE imaging data by using the program InsightSNAPS.<sup>23</sup> A paired *t* test was used for significant differences between the values at the gCC and sCC. A Mann-Whitney *U* test with a Bonferroni correction for multiple testing was used to compare the neighboring age groups in FA and T2 values (eg, 0–2 versus >2–5 years and >2–5 years versus >5–10 years). The age dependence of all the parameters was simulated with curve fits by using Origin software (OriginLab, Northampton, Mass).

## Results

**T2 Values.** The mean T2 values of the gCC and sCC (T2gCC and T2sCC) with their SDs for all subjects are depicted as data points with error bars versus age as indicated in Fig 2. Paired *t* tests show no significant difference between values of T2gCC and T2sCC ( $P > .05$ ). T2 values of both regions varied according to age in nearly the same manner, with the largest value of approximately 300 ms at the youngest age of 2 months. T2 values decreased continuously with increasing age, fast in the first year and slowly thereafter until the value of approximately 90 ms for the adult subjects. The relationship between T2 values and age could be fitted with a biexponential function (the solid line in Fig 2, upper part). As it is shown in Fig 2, no sex difference could be found.

**FA.** The mean FAGCC and FAsCC values with their SDs for all subjects versus age are depicted as data points with error bars as indicated in Fig 2. FA values of the 2 anatomic localizations show different age dependencies: The FAGCC increased continually from 0.48 to 0.80 (from 2 months to 5 years) and remained nearly constant thereafter. In contrast, the FAsCC values varied very little within the entire age range from 0.64 at 2 months of age to 0.80 at 2 years of age and then remained constant. A paired *t* test showed a significant difference between the values (FAGCC < FAsCC) until 5 years of age ( $P < .05$ ) and no significant difference in the later course. The FAGCC showed a significant increase between the age groups 0–2 versus 2–5 years ( $P < .001$ , Mann-Whitney *U* test), whereas there was no other difference between the other age groups. The age dependence of both FAs could be fitted with a monomolecular function—a biologic growth function:  $FA(t) = C_1 - C_2 e^{-kt}$ , where  $C_1$  (0.79 for gCC and 0.82 for sCC) and  $C_2$  (0.33 for gCC and 0.15 for sCC) are the initial constant and the amplitude of the dynamic term respectively,  $k$  (0.03/month for gCC and 0.01/month for sCC) is the growth ratio, and  $t$  is the age.<sup>24</sup> The results are shown in Fig 2. No significant difference was found between male and female subjects.

**Fiber Tracking and Volume Determination.** The fiber number of the CC (FNcc), a unitless number, versus age is drawn in Fig 3. As it is shown, FNcc increases continuously, fast in the age range of 2 months to 5 years (from 1500 to 10,000) and slowly thereafter. Meanwhile, the volume of CC (Vcc) shows a similar age dependence: It increases from approximately  $1000 \text{ mm}^3$  at 2 months of age to  $5000 \text{ mm}^3$  at 6 years of age and increases slowly after that. Curve fits of FNcc and Vcc values were made by using an asymptotic function:  $Y(t) = A - BC^t$ , where parameter  $A$  (10,000–13,900) is a constant;  $B$  (8200–9510) and  $C$  (0.990–0.993) are the amplitude and rate of the dynamic term respectively; and  $t$  is the age. The ratio of FNcc/Vcc (ie, the fiber density of the CC) is also given in Fig 3 (lower part), where a tendency of inverse age dependence from childhood to adulthood could be seen as fitted with a linear function. Although no differences between values of male and female children were found, independent *t* tests showed significant sex differences of FNcc and FNcc/Vcc of adults; accordingly, adult males tended to have a higher fiber number and fiber density than adult females ( $P < .05$ ).

The results are summarized in Figs 2 and 3, where the filled signs represent the values of the male subjects and the open signs, the female subjects. Curve fits for age dependence of all

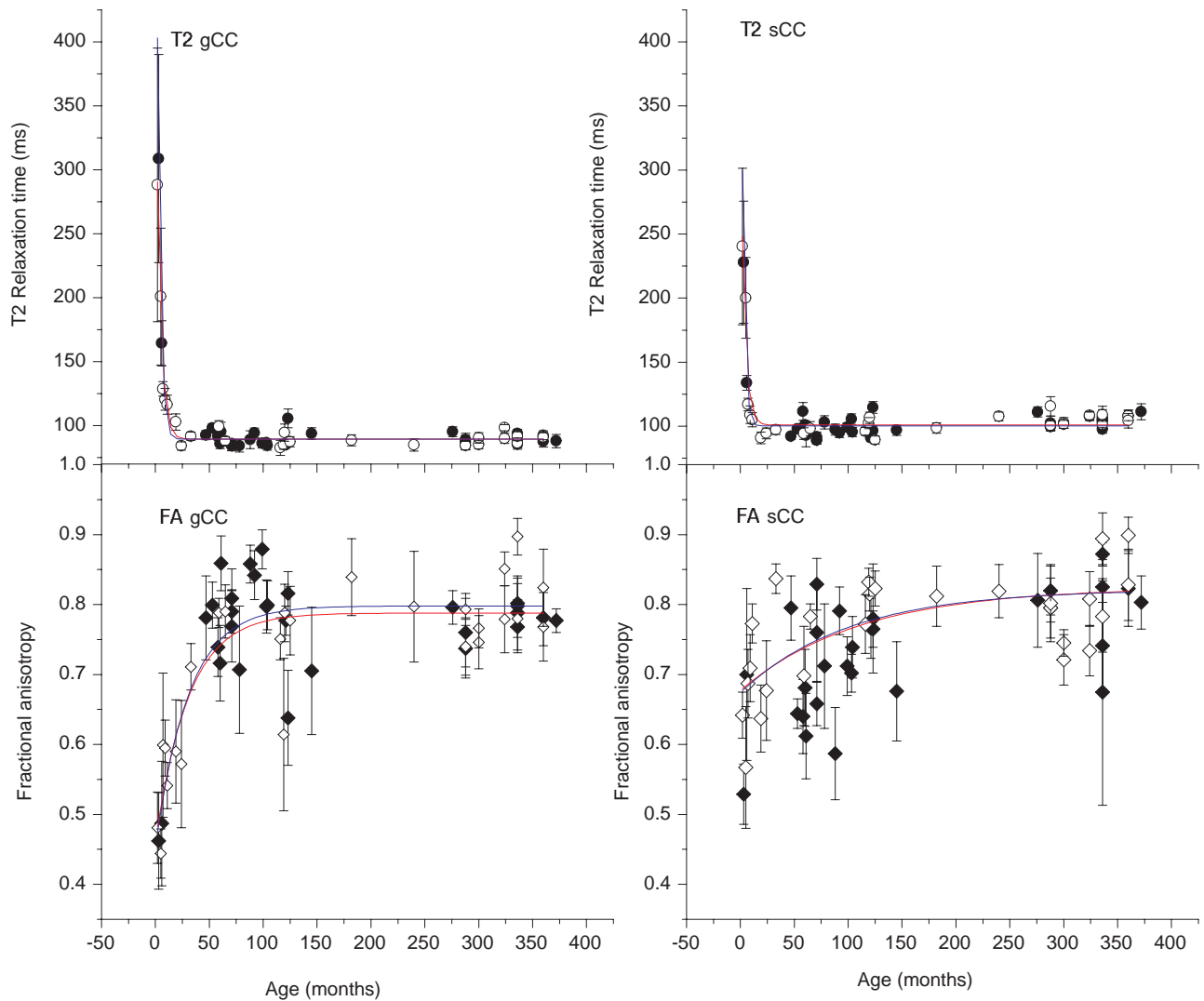


**Fig 2.** Numeric values and the corresponding curve fits of the T2 and FA values obtained at the regions of interest of the gCC and the sCC, respectively, where the filled signs represent the values of the male subjects and the open signs, the female subjects. The blue and the red solid lines are the corresponding fit results for male and female subjects.

the numeric parameters are carried out (solid lines, blue color for male subjects and red for female).

## Discussion

The present study was designed to investigate, in a routine clinical environment, the brain maturation beyond 2 years of age in a cohort representing a long time period of brain maturation. Therefore, more attention has been paid to lighten the burden for patients by minimizing the time the young patients spent in the magnet (eg, 6 motion-probing gradients were used in DTI, allowing a short scanning time of 3.5 minutes).<sup>21</sup> Second, to find out whether there are differences between measured values in male and female subjects, we drew these values separately according to the age in Figs 2 and 3. For neither T2 nor FA was significant sex difference found. However, we found significant sex differences in fiber number and fiber density of adults; adult males tended to have a higher fiber number and fiber density than adult females, in line with reports in the literature that the midsagittal cross-sectional area of the CC (CCA) was different for men and women (CCA men > CCA women).<sup>16,25</sup>

Diffusion anisotropy in white matter originates from its specific organization in bundles of more or less myelinated axonal fibers running in parallel. Diffusion in the direction of the fibers is faster than that in the perpendicular direction, though the exact mechanism is still not completely understood (ie, anisotropy is affected by both axon organization and myelination). As the brain maturation continues, different structures of the brain are more and more organized, especially the fiber tracts, which become more myelinated, inducing an increase of the spatial anisotropy.<sup>9</sup> Furthermore, brain maturation processes take place in different anatomic structures with different time courses. In a study on children from 8 to 12 years of age, Snook et al<sup>26</sup> found a linear age correlation of the FA of the CC, with a greater slope of increase for FAgCC than for FAsCC, indicating a more pronounced anterior development of the CC. The present observation of significant age-related increase in FA of the CC is consistent with that reported in other studies.<sup>8,27,28</sup> Especially, the present work confirms the findings of Snook et al,<sup>26</sup> with a decided age group within a larger time period: FAgCC and FAsCC values revealed different dynamics of age dependence. Starting with a

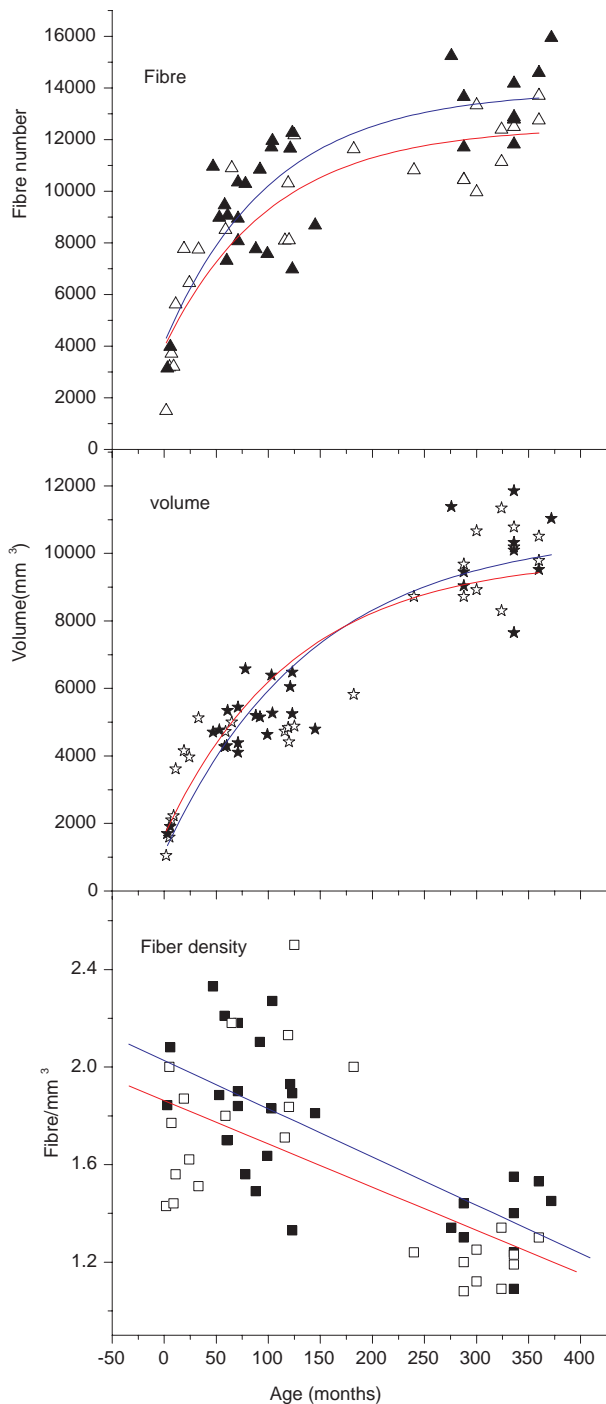


**Fig 3.** Numeric values and the corresponding curve fits of the fiber number, volume, and fiber attenuation of the CC, where the filled signs represent the values of the male subjects and the open signs, female subjects. The blue and the red solid lines are the corresponding fit results for male and female subjects.

value of 0.48 at 2 months of age, the FA<sub>gCC</sub> increases remarkably until 5 years of age, with a value of 0.8, and remains nearly constant thereafter. This unique increase of the FA<sub>gCC</sub> beyond 2 years of age is confirmed by the highly significant FA increase from 0–2 to >2–5 years that was not observed in FA<sub>sCC</sub>, where only a nonsignificant increase was found (from 0.64 to 0.8).

These observations may imply following: First, the maturation of gCC lags behind that of sCC at birth, following the

general myelination rule of posterior-anterior progression.<sup>29</sup> Second, an especially fast maturation takes place at the gCC postnatally with a period of rapid ongoing brain development much longer than that found by using quantitative T2 determination.<sup>2,5,7</sup> The results of the curve fit confirm this observation, where the initial constant  $C_1$  of the sCC is larger than that of gCC—an indication of less myelination of the gCC than that of the sCC at birth, whereas the dynamic amplitude  $C_2$  and the growth ratio  $k$  of gCC are larger than those of sCC, meaning a faster ongoing myelination process at gCC postnatally.

By determination of the CC volume, we found a continuous increase until adulthood, which is consistent with the work of Giedd et al,<sup>25</sup> who found a continued increase of the CC size through adolescence. The interpretation of the continuous increase of the absolute fiber number of the CC is at the moment unclear because electron microscopy studies of postnatal development of callosal axons in monkeys suggest no postnatal development of new callosal axons.<sup>13</sup> The cause is probably the increase of the myelination instead of the increase of the axons, which might be too complicated for the mathematic model of the fiber tracking to differentiate. Also an MR imaging scanner with higher field strength such as 3T may provide improved DTI tractography. Most interesting, on the basis of the results of fiber tracking and volumetry, we found a decreasing fiber density at the CC, with ongoing brain maturation suggesting “thicker” fiber bundles from infancy to adulthood (ie, the inverse relation of age and fiber density is caused by an increase in the relative amount of myelination).<sup>13</sup>

Childhood and adolescence are periods of dynamic behavioral, cognitive, and emotional development, which parallel significant changes in white matter structure. Callosal fibers are important for motor and sensory integration, attention, memory, and general cognitive functioning.<sup>10–12</sup> The time course of maturation until 5 years of age as observed in our study is concordant with major psychological maturation processes: The gCC is mainly related to important interhemispheric association fibers that play a major role in several of these processes. Any disturbance or anomalies in the CC can result in certain neurologic disorders.<sup>30–33</sup> Nevertheless, in the present work, the population between 2 and 5 years of age included only 7 children, a quite small sample size. A study with a larger number of subjects would be necessary to extract more reliable conclusions.

In conventional MR imaging, the myelination in hemispheric white matter is essentially complete by 24 months as determined usually by visual inspection of MR imaging based on the contrast variance shown in T1- and T2-weighted images.<sup>34</sup> More objective judgment of the myelination could be archived by using certain quantitative methods like T2 relaxation time measurement. T2 relaxation time of the human brain decreases during brain maturation, mainly due to increases in concentrations of the myelin basic protein and proteolipid protein and increases in macromolecules and the membrane surface-to-cell volume ratio and decrease in free water content.<sup>35,36</sup> After 20 months of age, only a minor T2 reduction was found as an indication of further brain maturation.<sup>7</sup> The present results of the measured T2 values at the CC are consistent with those reported for lobar white matter in maturing brains,<sup>4,6</sup> proving that the CC matures synchro-

nously with the lobar white matter. Additionally, with the DTI method in the present work, a rapid maturation process was observed in the gCC beyond 24 months of age, suggesting that DTI is a more sensitive method in detecting physiologic changes in brain maturation, as recently described by others.<sup>37</sup>

## Conclusion

The present work shows that rapid ongoing changes in brain maturation are detectable until 5 years of age. Although T2 measurements show nearly constant results beyond 2 years of age, DTI reveals rapid and highly significant ongoing changes in brain maturation (increase in FA in the genu of the callosal body) until 5 years of age. The FA measurement in the callosal body might be a useful auxiliary tool for visual inspection and T2 relaxometry, especially in children older than 2 years of age.

## References

1. Van der Knaap MS, Valk J. *Magnetic Resonance of Myelin, Myelination, and Myelin Disorders*. Berlin: Springer-Verlag; 2005
2. Holland BA, Haas DK, Norman D, et al. **MRI of normal brain maturation.** *AJNR Am J Neuroradiol* 1986;7:201–08
3. Miot-Noirault E, Barantin L, Akoka S, et al. **T2 relaxation time as a marker of brain myelination: experimental MR study in two neonatal animal models.** *J Neurosci Methods* 1997;72:5–14
4. Engelbrecht V, Rassek M, Preiss S, et al. **Age-dependent changes in magnetization transfer contrast of white matter in the pediatric brain.** *AJNR Am J Neuroradiol* 1998;19:1923–29
5. Papanikolaou N, Maniatis V, Pappas J, et al. **Biexponential T2 relaxation time analysis of the brain: correlation with magnetization transfer ratio.** *Invest Radiol* 2002;37:363–67
6. Ding XQ, Wittkugel O, Goebell E, et al. **Clinical applications of quantitative T2 determination: a complementary MRI tool for routine diagnosis of suspected myelination disorders.** *Eur J Paediatr Neurol* 2007 Oct 25 [Epub ahead of print]
7. Ding XQ, Kucinski T, Wittkugel O, et al. **Normal brain maturation characterized with age-related T2 relaxation times: an attempt to develop a quantitative imaging measure for clinical use.** *Invest Radiol* 2004;39:740–46
8. Barnea-Goraly N, Menon V, Eckert M, et al. **White matter development during childhood and adolescence: a cross-sectional diffusion tensor imaging study.** *Cereb Cortex* 2005;15:1848–54. Epub 2005 Mar 9
9. Ben Bashat D, Ben Sira L, Graif M, et al. **Normal white matter development from infancy to adulthood: comparing diffusion tensor and high b value diffusion weighted MR images.** *J Magn Reson Imaging* 2005;21:503–11
10. Bookstein FL, Streissguth AP, Sampson PD, et al. **Corpus callosum shape and neuropsychological deficits in adult males with heavy fetal alcohol exposure.** *Neuroimage* 2002;15:233–51
11. Brown WS, Jeeves MA, Dietrich R, et al. **Bilateral field advantage and evoked potential interhemispheric transmission in commissurotomy and callosal agenesis.** *Neuropsychologia* 1999;37:1165–80
12. Eliassen JC, Baynes K, Gazzaniga MS. **Anterior and posterior callosal contributions to simultaneous bimanual movements of the hands and fingers.** *Brain* 2000;123(Pt 12):2501–11
13. LaMantia AS, Rakic P. **Axon overproduction and elimination in the corpus callosum of the developing rhesus monkey.** *J Neurosci* 1990;10:2156–75
14. Kier EL, Truwit CL. **The normal and abnormal genu of the corpus callosum: an**

- evolutionary, embryologic, anatomic, and MR analysis. *AJNR Am J Neuroradiol* 1996;17:1631–41
15. Barkovich AJ. **Analyzing the corpus callosum.** *AJNR Am J Neuroradiol* 1996;17:1643–45
16. Mitchell TN, Free SL, Merschhemke M, et al. **Reliable callosal measurement: population normative data confirm sex-related differences.** *AJNR Am J Neuroradiol* 2003;24:410–18
17. McLaughlin NC, Paul RH, Grieve SM, et al. **Diffusion tensor imaging of the corpus callosum: a cross-sectional study across the lifespan.** *Int J Dev Neurosci* 2007;25:215–21. Epub 2007 Apr 1
18. Klingberg T, Vaidya CJ, Gabrieli JD, et al. **Myelination and organization of the frontal white matter in children: a diffusion tensor MRI study.** *Neuroreport* 1999;10:2817–21
19. Gilmore JH, Lin W, Corouge I, et al. **Early postnatal development of corpus callosum and corticospinal white matter assessed with quantitative tractography.** *AJNR Am J Neuroradiol* 2007;28:1789–95
20. Basser PJ, Pierpaoli C. **A simplified method to measure the diffusion tensor from seven MR images.** *Magn Reson Med* 1998;39:928–34
21. Okada T, Miki Y, Kikuta K, et al. **Diffusion tensor fiber tractography for arteriovenous malformations: quantitative analyses to evaluate the corticospinal tract and optic radiation.** *AJNR Am J Neuroradiol* 2007;28:1107–13
22. Jiang H, van Zijl PC, Kim J, et al. **DTIStudio: resource program for diffusion tensor computation and fiber bundle tracking.** *Comput Methods Programs Biomed* 2006;81:106–16. Epub 2006 Jan 18
23. Yushkevich PA, Piven J, Hazlett HC, et al. **User-guided 3D active contour segmentation of anatomical structures: significantly improved efficiency and reliability.** *Neuroimage* 2006;31:1116–28. Epub 2006 Mar 20
24. Seber GAF, Wild CJ. *Nonlinear Regression*. New York: Wiley; 2003
25. Giedd JN, Blumenthal J, Jeffries NO, et al. **Development of the human corpus callosum during childhood and adolescence: a longitudinal MRI study.** *Prog Neuropsychopharmacol Biol Psychiatry* 1999;23:571–88
26. Snook L, Paulson LA, Roy D, et al. **Diffusion tensor imaging of neurodevelopment in children and young adults.** *Neuroimage* 2005;26:1164–73
27. Engelbrecht V, Scherer A, Rassek M, et al. **Diffusion-weighted MR imaging in the brain in children: findings in the normal brain and in the brain with white matter diseases.** *Radiology* 2002;222:410–18
28. Hermoye L, Saint-Martin C, Cosnard G, et al. **Pediatric diffusion tensor imaging: normal database and observation of the white matter maturation in early childhood.** *Neuroimage* 2006;29:493–504. Epub 2005 Sep 27
29. Rademacher J, Engelbrecht V, Burgel U, et al. **Measuring in vivo myelination of human white matter fiber tracts with magnetization transfer MR.** *Neuroimage* 1999;9:393–406
30. Baumgardner TL, Singer HS, Denckla MB, et al. **Corpus callosum morphology in children with Tourette syndrome and attention deficit hyperactivity disorder.** *Neurology* 1996;47:477–82
31. Mostofsky SH, Wendlandt J, Cutting L, et al. **Corpus callosum measurements in girls with Tourette syndrome.** *Neurology* 1999;53:1345–47
32. MacKay A, Laule C, Vavasour I, et al. **Insights into brain microstructure from the T2 distribution.** *Magn Reson Imaging* 2006;24:515–25. Epub 2006 Mar 20
33. Narberhaus A, Segarra D, Caldu X, et al. **Corpus callosum and prefrontal functions in adolescents with history of very preterm birth.** *Neuropsychologia* 2008; 46:111–16. Epub 2007 Aug 10
34. Barkovich AJ. *Pediatric Neuroimaging*. Philadelphia: Lippincott Williams & Wilkins; 2005
35. Tower DB, Bourke RS. **Fluid compartmentation and electrolytes of cat cerebral cortex in vitro. 3. Ontogenetic and comparative aspects.** *J Neurochem* 1966;13:1119–37
36. Morell P, Quarles RH, Norton WT. **Myelin formation: structure, and biochemistry.** In: Siegel GJ, ed. *Basic Neurochemistry: Molecular, Cellular and Medical Aspects*. 5th ed. New York: Raven Press; 1994;117–43
37. Giorgio A, Watkins KE, Douaud G, et al. **Changes in white matter microstructure during adolescence.** *Neuroimage* 2008;39:52–61. Epub 2007 Aug 11